Evidence in neutrino scattering for right-handed currents associated with heavy quarks*

R. Michael Barnett

Lyman Laboratory of Physics, Harvard University, Cambridge, Massachusetts 02138
(Received 23 January 1976)

The production of heavy quarks is considered in the quark-parton model. The model is shown to account for the energy-dependent effects of large produced masses. By considering the inclusive, charged-current neutrino scattering data as a function of energy, it is possible to distinguish between the standard four-quark model and models with right-handed currents and additional heavy quarks. It appears that the present data favor the latter models, and allow estimates of the masses of new quarks.

I. INTRODUCTION

The experiments of the Harvard-Pennsylvania-Wisconsin-Fermilab (HPWF), Caltech-Fermilab (CTF), and CERN Gargamelle collaborations have found several exciting phenomena. These experiments have neutrino and antineutrino beams which collide with nucleii with approximately equal mixtures of neutrons and protons and therefore with equal numbers of u and d quarks.

In theories with a charged intermediate boson (W), the ν $(\bar{\nu})$ is changed into a μ^- (μ^+) at the leptonic vertex and hadrons are created at the other vertex. The production of muons by neutrinos has been observed[1-4]. In addition these groups discovered neutral-current events[1,5,6] in which no muon is created, but those events are not directly relevant to the discussion here and are not considered.

The quark-parton model has clear predictions for the total cross sections and for several distributions which were confirmed by the early experiments at low energies.[1-3] Later, however, HPWF reported an anomaly in one distribution[7] at higher energies which still persists.[8]

Recently HPWF[9-12] and CTF[13] have reported events in which a second muon, usually of opposite charge, is found. The second muon appears to come not from the leptonic vertex,[14-16] but from the hadronic vertex, presumably from the weak decay of heavy particles, which will be called charmed particles here.

In the old quark model one expected that in ν $(\bar{\nu})$ scattering W^+ (W^-) bosons would change d (u) quarks into u (d) quarks. In that process only ordinary light particles would be produced. However, in what is now referred to as the standard model[17] there are four quarks with the left-handed couplings:

$$\begin{pmatrix} u \\ d_C \end{pmatrix}_L \quad \begin{pmatrix} c \\ s_C \end{pmatrix}_L$$

$$(1.1)$$

or

$$J_\mu^{\text{charged}} = \bar{u}\gamma_\mu(1+\gamma_5)d_C + \bar{c}\gamma_\mu(1+\gamma_5)s_C \quad (1.2)$$

where

$$\begin{aligned} d_C &\equiv d\cos\theta_C + s\sin\theta_C \\ s_C &\equiv -d\sin\theta_C + s\cos\theta_C \end{aligned} \quad (1.3)$$

and $\tan^2\theta_C \approx 0.05$. In this model strange quarks which are found in the sea of nucleons can be changed into charmed quarks c (the sea is quark-antiquark pairs found in addition to the valence u and d quarks).

Following the discovery[18,19] of the ψ_J and in the light of the HPWF and CTF experiments, several new models were proposed. Among these models[20-27] many had right-handed currents and several had additional heavy quarks.

One of the problems with models which have right-handed couplings such as $(u,d')_R$ is that the $\bar{\nu}$ cross section is predicted to rise by a factor of four (over the usual cross section) after passing the threshold energy for producing particles with a quark d'. No rise of that magnitude has been observed. However, as was discussed[28] before these phenomena were found, the effects of new heavy quarks may be slow to reach their asymptotic levels.

Here it will be shown that the ordinary quark-parton model provides a description of the rate of approach to the asymptotic limit when the mass of the produced quark is kept. This approach allows an estimation of the mass of the relevant quarks when the data are considered in the context of a variety of models. No other masses (such as light-quark masses or nucleon masses) significantly affect the results.

The energy-dependent cross sections are derived in Sec. II, where it is shown how the produced-quark mass enters in the quark-parton model. The qualitative effects of a heavy-produced-quark mass, discussed in Sec. III, include the suppression of large x and small y. In Sec. IV the models tested are described, and the form of valence- and

sea-quark distributions used are given. The results of comparing a variety of models with the data are presented in Sec. V along with the conclusions.

These and other aspects of charged-current neutrino scattering have also been considered in Refs. 29 and 30.

II. CROSS SECTIONS FOR PRODUCTION OF HEAVY QUARKS

A. Scaling behavior with heavy quarks

In the quark-parton model, it is assumed that the exchanged W boson in νN scattering interacts with one of the constituent quarks of the nucleon. This quark carries a fraction z of the nucleon's total momentum where the distribution of these fractions is described by the structure functions $F(z)$. It is further assumed that these quark-partons are quasifree[31] so that the impulse approximation is valid. In this approximation the produced quark c is on mass shell so that if the quark c is light one obtains from Fig. 1

$$(q + zp)^2 = p'^2 \approx 0, \tag{2.1}$$

$$q^2 + 2zq \cdot p + z^2 M^2 \approx 0.$$

Neglecting the last term,

$$z \approx \frac{-q^2}{2p \cdot q} \equiv x. \tag{2.2}$$

The term $-q^2/2p \cdot q$, which is generally called x, is an experimentally observable quantity.

However, if the quark c has non-negligible mass $(m_c \gg 0.3 \text{ GeV})$ then

$$(q + zp)^2 = p'^2 = m_c^2, \tag{2.3}$$

and

$$z = \frac{-q^2 + m_c^2}{2p \cdot q} = x\left(\frac{-q^2 + m_c^2}{-q^2}\right), \tag{2.4}$$

or

$$z = x + \frac{m_c^2}{2MEy}, \tag{2.5}$$

where

$$y = \frac{E - E'}{E} \quad (k_0 = E \text{ and } k_0' = E');$$

y is also observable experimentally.

The result of this parton calculation[32] is that the scaling variable z is not equal to the experimental variable x of heavy quarks are produced. Therefore, x and z must be kept distinct in calculating the cross section.

Because one is connecting this quark mass m_c with the threshold behavior of the cross section, it is reasonable that such masses should have an approximate correspondence with the masses of the hadrons of which they are constituents.

B. Calculation of cross section without parton hypothesis

In order to show clearly the role of heavy quarks, it will be useful to recalculate the standard cross sections.[33] For the νN scattering shown in Fig. 1, the matrix element is

$$\mathfrak{M} = \frac{G}{\sqrt{2}} \bar{u}_\mu \gamma_\alpha (1 - \gamma_5) u_\nu \langle X | J_{ch}^\alpha | N \rangle \tag{2.6}$$

and the cross section is

$$\frac{d^2\sigma}{dE'd\Omega'} = \frac{G^2}{2} \frac{E'}{E} \frac{m_\mu m_\nu}{(2\pi)^2} l_{\alpha\beta} W^{\alpha\beta}, \tag{2.7}$$

where the leptonic part is

$$l_{\alpha\beta} = \sum \bar{u}\gamma_\alpha(1 - \gamma_5) u \bar{u}\gamma_\beta(1 - \gamma_5) u$$

$$= \frac{2}{m_\mu m_\nu} \left[k_\alpha' k_\beta + k_\beta' k_\alpha - k \cdot k' g_{\alpha\beta} \mp i\epsilon_{\alpha\beta\gamma\delta} k^\gamma k'^\delta \right] \tag{2.8}$$

and the hadronic part is

$$W^{\alpha\beta} = \frac{1}{2} \sum \sum_X \langle N | J_{ch}^{\dagger\beta} | X \rangle \langle X | J_{ch}^\alpha | N \rangle (2\pi)^3$$

$$\times \delta^4(p + q - p_X). \tag{2.9}$$

When $W^{\alpha\beta}$ is multiplied by $l_{\alpha\beta}$, certain terms in $W^{\alpha\beta}$ (W_4 and W_5) are multiplied by m_μ. In this type of theory one also finds $W_6 = 0$. Neglecting W_4, W_5, and W_6, the most general allowed $W^{\alpha\beta}$ is

$$W^{\alpha\beta} = -g^{\alpha\beta} W_1 + \frac{p^\alpha p^\beta}{M^2} W_2 + i\epsilon^{\alpha\beta\gamma\delta} \frac{p_\gamma p_\delta}{2M^2} W_3. \tag{2.10}$$
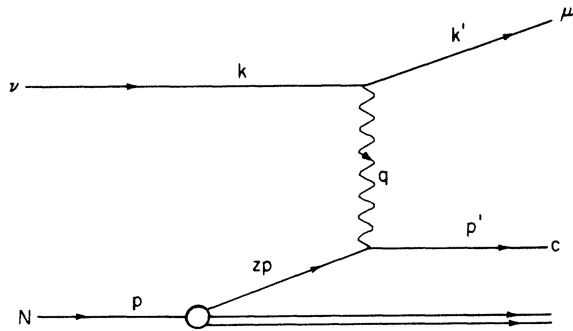

FIG. 1. A quark-parton picture of the νN scattering in which a quark c is produced with the exchange of a W boson. The recombination of quarks to form hadrons is not shown.

Using the scaling hypothesis, the W_i can be equated with scaling functions F_i which are functions only of the scaling variable z:

$$F_1 = W_1 M, \quad F_2 = \nu W_2, \quad F_3 = \nu W_3, \tag{2.11}$$

so that

$$W^{\alpha\beta} = -\frac{g^{\alpha\beta}}{M}F_1 + \frac{p^{\alpha}p^{\beta}}{M^2\nu}F_2 + i\epsilon^{\alpha\beta\gamma\delta}\frac{p_{\gamma}q_{\delta}}{2M^2\nu}F_3. \tag{2.12}$$

Then multiplying $l_{\alpha\beta}$ by $W^{\alpha\beta}$ in the cross section, Eq. (2.7),

$$\frac{d^2\sigma}{dE'd\Omega'} = \frac{G^2E'2}{2E(2\pi)^2}\left[F_1\left(\frac{2k\cdot k'}{M}\right)+\frac{F_2}{\nu}\left(\frac{2(p\cdot k)(p\cdot k')}{M^2}-k\cdot k'\right)\pm\frac{F_3}{\nu}\left(\frac{(\delta_{\gamma}{}^{\mu}\delta_{\delta}{}^{\nu}-\delta_{\gamma}{}^{\nu}\delta_{\delta}{}^{\mu})k^{\gamma}k'^{\delta}p_{\mu}q_{\nu}}{M^2}\right)\right]. \tag{2.13}$$

Writing this cross section in the lab frame (N at rest)

$$\frac{d^2\sigma}{dE'd\Omega'} = \frac{G^2E'^2}{2\pi^2}\left[\frac{2}{M}\sin^2\frac{\theta}{2}F_1+\cos^2\frac{\theta}{2}\frac{F_2}{\nu}\right.$$

$$\left.\mp\frac{E+E'}{M}\sin^2\frac{\theta}{2}\frac{F_3}{\nu}\right]. \tag{2.14}$$

This can be written in terms of the variables x and y:

$$x \equiv \frac{-q^2}{2p\cdot q}, \quad y \equiv \frac{E-E'}{E}, \tag{2.15}$$

where

$$p\cdot q = M\nu = M(E-E') = MEy, \quad -q^2 = 2MExy.$$

$$\sin^2\frac{\theta}{2} = \frac{Mxy}{2E'} = \frac{Mxy}{2E(1-y)}, \tag{2.16}$$

$$\frac{d^2\sigma}{dxdy} = \frac{2\pi MEy}{E'}\frac{d^2\sigma}{dE'd\Omega'} = \frac{2\pi My}{(1-y)}\frac{d^2\sigma}{dE'd\Omega'}.$$

Then

$$\frac{d^2\sigma}{dxdy} = \frac{G^2ME}{\pi}[xy^2F_1+(1-y)F_2\mp(1-\tfrac{1}{2}y)xyF_3], \tag{2.17}$$

where a term $(F_2Mxy/2E)$ has been neglected.

C. Cross section from quark-parton model

Within the quark-parton model $W^{\alpha\beta}$ can be calculated more explicitly in terms of the scaling variable z,

$$z = x + \frac{m_c^2}{2MEy}. \tag{2.18}$$

For ν scattering, only the d quark contributes (for simplicity we ignore sea contributions here) so that

$$W^{\alpha\beta} = d(z)h^{\alpha\beta}\theta(1-z), \tag{2.19}$$

where

$$h^{\alpha\beta} \propto \sum \sum_i \langle zp|J^{\dagger\beta}|p_i'\rangle\langle p_i'|J^{\alpha}|zp\rangle\delta^4(p'-q-zp) \tag{2.20}$$

$$\propto \text{Tr}[(z\not{p})\gamma^{\beta}(1-\gamma_5)(z\not{p}+\not{q})\gamma^{\alpha}(1-\gamma_5)]. \tag{2.21}$$

Doing the trace and neglecting the W_5-type term and a z^2M^2 term, one obtains

$$h^{\alpha\beta} \propto M\nu z\left(-g^{\alpha\beta}+\frac{2z}{M\nu}p^{\alpha}p^{\beta}-i\frac{\epsilon^{\alpha\beta\gamma\delta}}{M\nu}p_{\gamma}q_{\delta}\right). \tag{2.22}$$

From this, $W^{\alpha\beta}$ can be obtained after inserting the correct normalization.

$$W^{\alpha\beta} = d(z)\left(-\frac{g^{\alpha\beta}}{M}+\frac{2z}{M^2\nu}p^{\alpha}p^{\beta}-i\frac{\epsilon^{\alpha\beta\gamma\delta}}{M^2\nu}p_{\gamma}q_{\delta}\right)\theta(1-z). \tag{2.23}$$

By comparing with Eq. (2.12), it follows that

$$F_1 = d(z), \tag{2.24}$$

$$F_2 = 2zd(z) = 2zF_1, \tag{2.25}$$

$$F_3 = -2d(z) = -F_2/z. \tag{2.26}$$

The relation Eq. (2.25) is the Callan-Gross relation.[34]

Substituting these relations into Eq. (2.17), the final cross section is obtained:

$$\frac{d^2\sigma}{dxdy} = \frac{G^2ME}{\pi}\left\{(1-y)+\frac{x}{z}\left[\tfrac{1}{2}y^2\pm(y-\tfrac{1}{2}y^2)\right]\right\}$$

$$\times F_2(z)\theta(1-z), \tag{2.27}$$

where $\pm$ refers to ν or $\bar{\nu}$ for left-handed currents. Note that for $m_c \to 0$ ($z \to x$), the standard result is found:

$$\left.\frac{d^2\sigma}{dxdy}\right|_{m_c=0} = \frac{G^2ME}{\pi}F_2(x)\times\begin{cases}1, & \text{for }\nu, \\ (1-y)^2, & \text{for }\bar{\nu}.\end{cases} \tag{2.28}$$

In Eq. (2.27), the actual threshold is described not by $\theta(1-z)$ but by $\theta(1-z')$, where z' is the same as z except for replacing m_c^2 with $W_{\min}^2-M^2$. However,

it is z, not z', which enters elsewhere, and it can be shown that either θ function gives similar results when Eq. (2.27) is used with z.

III. QUALITATIVE IMPLICATIONS OF CHARM CROSS SECTIONS

From the fact that $z \leqslant 1$ and the use of Eq. (2.5), there are bounds set on x and y:

$$x \leqslant 1 - \frac{m_c^2}{2MEy} \leqslant 1 - \frac{m_c^2}{2ME}, \tag{3.1}$$

$$y \geqslant \frac{m_c^2}{2ME(1-x)} \geqslant \frac{m_c^2}{2ME}. \tag{3.2}$$

If these bounds are violated, then the production of a quark of mass m_c is kinematically forbidden. An equivalent bound exists for the scaling variable z:

$$z \geqslant \frac{m_c^2}{2MEy} \geqslant \frac{m_c^2}{2ME} \tag{3.3}$$

If one considers $m_c = 4$ GeV, then for $y = 0.5$, $x \leqslant 0.6$, and for $x = 0.25$, $y \geqslant 0.27$ (for $E = 40$ GeV).

In the cross section Eq. (2.27), the heavy-quark mass has three effects at finite energies: (1) The magnitude of the cross section is decreased for all x and y; (2) The x distribution is modified by suppressing large x relative to small x; (3) The y distribution is modified by the suppression of small y.

The most dramatic effects occur in $F_2(z)$. Assume that

$$F_2(z) = (1-z)^3 = \left(1 - x - \frac{m_c^2}{2MEy}\right)^3. \tag{3.4}$$

Since experimental distributions are plotted versus x, not z, it is clear that with increasing m_c the magnitude of F_2 decreases significantly, and F_2 falls off more rapidly in x. Furthermore, as y is decreased, F_2 decreases. Clearly all three of these effects are magnified for higher powers of $1-z$. Higher powers are expected for sea contributions (quark-antiquark pairs present in the nucleon). This last effect is shown in Fig. 2.

The presence of the factor x/z in the cross section, Eq. (2.27), also has significant effects. This factor enters because there are kinematical factors x in the cross section [see Eq. (2.17)] and because the relations Eqs. (2.25) and (2.26), which are obtained in the parton model, contain the scaling variable z. Since x/z is always less than one, it decreases the cross section. It also makes the second and third terms in Eq. (2.27) smaller relative to the first. As a result, distributions which otherwise would be proportional to 1 or to $(1-y)^2$ are both more like $1-y$. This effect is greatest for small x and for small y, where x/z is smallest.
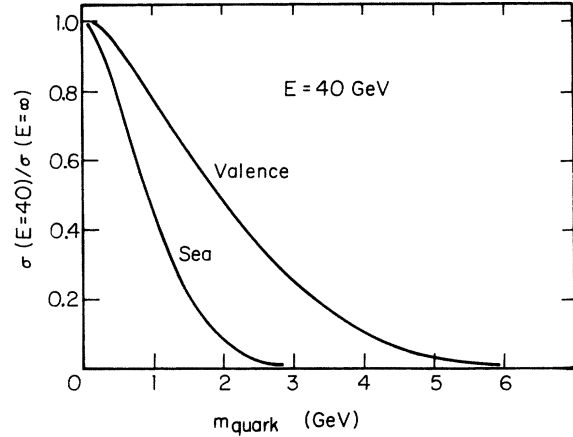

FIG. 2. An example of the suppression of cross sections when heavy quarks are produced, which is a function of whether a valence or sea quark was hit by the W boson.

The factor x/z tends to suppress small y.

Finally, since the x and y dependences no longer factorize, efficiencies which vary as a function of y now also affect the x dependences. Given the efficiency of the HPWF experiment[7] (poor efficiency at large y), one finds that for heavy-quark production, the x distributions are significantly more peaked at small x than they would be if the efficiency were not y dependent. These effects are magnified for those distributions which are peaked toward large y. However, in the theoretical distributions which follow, this effect is not included, since the experiments to be done in the near future will not have these efficiency problems.

IV. MODELS AND OTHER ASSUMPTIONS

A variety of quark models were compared with the data. Except for the standard four-quark model, the models considered here all have both left- and right-handed currents. Other models were examined but were found difficult to distinguish from the models considered. For many of the distributions which follow, it was also difficult to distinguish among the various nonstandard models for similar masses so that only one such model plus the standard model are shown. What is clearly evident is the presence or absence of the weak couplings:

$$\begin{pmatrix} u \\ d' \end{pmatrix}_R \text{ and } \begin{pmatrix} u' \\ d \end{pmatrix}_R, \tag{4.1}$$

where d' and u' signify any heavy quark which couples weakly to u or d quarks. In particular, this approach does not distinguish $(c,d)_R$ from $(u',d)_R$. However, this approach does give the approximate

masses of the u' and d' quarks [as defined in Eq. (4.1)].

The models considered are shown in Table I, where no Cabibbo angles are shown, although the standard Cabibbo angle was used in all models.

In order to calculate in each model, an assumption was required as to the magnitude and z dependence of the valence- and sea-quark distributions. For the results shown in Sec. V, the following distributions were assumed:

Valence: $\quad F_2^V(z) = (1 - z)^3 - 0.6(1 - z)^7,$ \quad (4.2)

Sea: $\quad F_2^S(z) = 0.19(1 - z)^9.$ \quad (4.3)

These give a ratio of the sea to valence contributions of 11% for all z [obtained by integrating $F_2(z)$ over z] and of 29% for $z < 0.1$ (recall that below charm threshold $x \simeq z$). Also shown in the theoretical results are the predictions of the models with one-fifth as much sea [in Eq. (4.3), $0.19 \to 0.04$].

The detailed shape of the distributions Eqs. (4.2) and (4.3) are not important to the results. The valence distribution was varied by changing the factor 0.6 (including changing it to zero); and the sea distribution was varied by trying different powers of $(1 - z)$ and other forms [including $(1 - z)^7$ and $\exp(-az^2)$]. These modifications had no qualitative importance on the features described and very little quantitative relevance for parameterizations consistent with the data. Parameterizations which have the valence distribution going to zero at *very* small x (those in Ref. 30 were used) change little

since the contribution of a small region is small. If the valence distribution $(1 - z)^3$ is changed to $(1 - z)^4$, the features of heavy-quark production described in Sec. III are, of course, magnified somewhat.

An important assumption in these calculations was that the number of strange quarks in the sea is equal to the number of $\bar{u}$ and $\bar{d}$ quarks in the sea; this is discussed further in the next section. It was also assumed that there were no charmed quarks in the sea.

V. RESULTS AND CONCLUSIONS

In comparing data and theory (as below), it was evident that if there is a $(u, d')_R$ coupling, the d' quark could not have a mass much less than 4 GeV. The best fits were obtained for a mass

$$m(d') \simeq 4 \text{ to } 5 \text{ GeV}. \qquad (5.1)$$

For a u' quark with a $(u', d)_R$ coupling, the present data are less conclusive and one cannot rule out masses between 2 and 4 GeV (masses much above 4 GeV make the models difficult to distinguish from the standard model). The best fits were obtained for masses

$$m(u') \gtrsim 3 \text{ GeV}. \qquad (5.2)$$

In the discussion which follows, the results are usually presented in terms of model A, but similar results can be obtained in model B. In model D there is no u' quark although there is a d' quark,

TABLE I. The weak couplings of the models considered. Primes denote heavy quarks. Cabibbo angles are not shown here, but were included in all calculations. Most of the models below also describe leptons which are not shown (see Ref. 22).

Model	Couplings	References
Standard	$\begin{pmatrix} u \\ d \end{pmatrix}_L \begin{pmatrix} c \\ s \end{pmatrix}_L$	17
A	$\begin{pmatrix} u \\ d \end{pmatrix}_L \begin{pmatrix} c \\ s \end{pmatrix}_L \begin{pmatrix} u' \\ d' \end{pmatrix}_L \quad \begin{pmatrix} u' \\ d \end{pmatrix}_R \begin{pmatrix} c \\ s \end{pmatrix}_R \begin{pmatrix} u \\ d' \end{pmatrix}_R$	24–27
B	$\begin{pmatrix} u \\ d \end{pmatrix}_L \begin{pmatrix} c \\ s \end{pmatrix}_L \begin{pmatrix} u' \\ d' \end{pmatrix}_L \quad \begin{pmatrix} c \\ d \end{pmatrix}_R \begin{pmatrix} u' \\ s \end{pmatrix}_R \begin{pmatrix} u \\ d' \end{pmatrix}_R$	24
C	$\begin{pmatrix} u \\ d \end{pmatrix}_L \begin{pmatrix} c \\ s \end{pmatrix}_L \quad \begin{pmatrix} c \\ d \end{pmatrix}_R$	23
D	$\begin{pmatrix} u \\ d \end{pmatrix}_L \begin{pmatrix} c \\ s \end{pmatrix}_L \quad \begin{pmatrix} u \\ d' \end{pmatrix}_R \begin{pmatrix} c \\ s' \end{pmatrix}_R$	20–22
E	$\begin{pmatrix} u \\ d \end{pmatrix}_L \begin{pmatrix} c \\ s \end{pmatrix}_L \begin{pmatrix} u' \\ d' \end{pmatrix}_L \begin{pmatrix} c' \\ s' \end{pmatrix}_L \quad \begin{pmatrix} u' \\ d \end{pmatrix}_R \begin{pmatrix} c' \\ s \end{pmatrix}_R \begin{pmatrix} u \\ d' \end{pmatrix}_R \begin{pmatrix} c \\ s' \end{pmatrix}_R$	22

and this possibility cannot be ruled out by the data.

To calculate the theoretical rate of dimuon production compared to single-muon production, one must first calculate the rate of charmed-quark production compared to light-quark production. This is done in the manner described in Sec. II. But, in addition, one must know the branching ratio of charmed particles to muons:

$$B_\mu \equiv \Gamma(D \to \mu + \text{anything})/\Gamma(D \to \text{anything}), \quad (5.3)$$

so that

$$\sigma(\nu N \to \mu\mu + \text{anything}) = B_\mu \sigma(\nu N \to D + \text{anything}). \quad (5.4)$$

Since $\sigma(D)$ can be obtained theoretically (Sec. II) and $\sigma(\mu\mu)$ is known experimentally, one can find the value of B_μ required for each model to agree with experiment.

These values of B_μ are shown in Table II for a variety of possible masses and amounts of sea in the nucleon. Naively one might expect $B_\mu \simeq 20\%$ since in the decay of a charmed particle the W boson can couple equally to $\mu - \nu$, $e - \nu$, and $u - d$ (in three colors). However, with certain model-dependent assumptions, Gaillard, Lee, and Rosner[35] have estimated $B_\mu \simeq 4\%$. Here it is assumed only that $B_\mu \lesssim 20\%$.

In order to obtain reasonable values for B_μ in the standard four-quark model, it was necessary to choose several parameters ideally: (1) The amount of sea assumed was 11% (29% at $x < 0.1$); it is difficult to have a larger sea contribution and still be consistent with low-energy data, but there could be a smaller sea contribution; (2) It was assumed that the amount of strange quarks in the sea is equal to the number of $\bar{u}$ and $\bar{d}$ quarks in the

sea; while there is no clear experimental evidence on this question, it has been argued by some that in the sea $s/\bar{u} \simeq \frac{1}{3}$; (3) The mass of the c quark was chosen as 1.5 GeV; few would argue that it is lighter. Both the HPWF and CTF groups have been very conservative in their estimates of dimuon production. Any of the above could double or triple the values of B_μ given for the standard model in Table II.

However, given the above assumptions one does obtain plausible values for $B_\mu(\nu)$ and $B_\mu(\bar{\nu})$ in the standard four-quark model.

Reasonable values for B_μ are obtained in most of the other models shown. For model C the discrepancy between $B_\mu(\nu)$ and $B_\mu(\bar{\nu})$ is quite large even considering the experimental error [note that the branching ratio to muons may be different for charmed mesons and charmed baryons, and only ν (not $\bar{\nu}$) produce charmed baryons in this model].

One of the more dramatic effects observed in the HPWF experiment[8] has been the change with energy in the average value of $y \equiv (E - E')/E$ for the process $\bar{\nu} + N \to \mu^+ + \text{anything}$. In Fig. 3 the data for $\langle y \rangle$ vs. E is shown along with the results for the standard model and for model A with various masses and amounts of sea. Because of some experimental limitations in the present data, certain small systematic errors are possible which shift all points in an energy-independent manner, but the magnitude of any energy-dependent errors is expected to be much smaller than the observed effect.
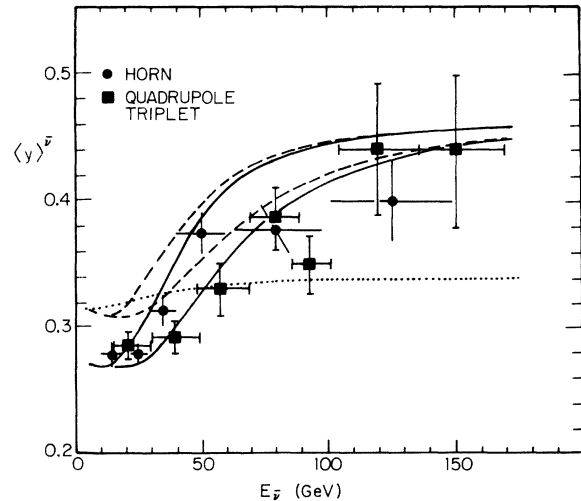
The standard four-quark model does very poorly

TABLE II. The branching ratio B_μ of charmed particles to muons [see Eq. (5.3)] required for each model to fit the observed dimuon rate, Refs. 10, 12, and 13. The ratios B_μ given are only good to 33% for ν and 50% for $\bar{\nu}$, since that is the current experimental error for $\sigma(\nu \to \mu\mu)$. Model B has similar results to model A.

Model	$B_\mu(\nu)$	$B_\mu(\bar{\nu})$	Quark masses (GeV)			% of sea
Standard	0.13	0.21	$c = 1.5$			11
A	0.06	0.04	$c = 1.5$	$u' = 4$	$d' = 4$	11
A	0.08	0.08	$c = 1.5$	$u' = 4$	$d' = 5$	11
A	0.05	0.06	$c = 4$	$u' = 2$	$d' = 4$	11
A	0.05	0.12	$c = 4$	$u' = 2$	$d' = 5$	11
A	0.08	0.04	$c = 1.5$	$u' = 4$	$d' = 4$	2
A	0.12	0.09	$c = 1.5$	$u' = 4$	$d' = 5$	2
A	0.05	0.04	$c = 4$	$u' = 2$	$d' = 4$	2
A	0.05	0.10	$c = 4$	$u' = 2$	$d' = 5$	2
C	0.03	0.16	$c = 1.5$			11
D	0.13	0.04	$c = 1.5$		$d' = 4$	11
D	0.13	0.08	$c = 1.5$		$d' = 5$	11

FIG. 3. The average value of y in the distributions for $\bar{\nu} N \to \mu^+ X$. Data are from Ref. 8. The curves are predictions for the standard model (dotted) and for model A with 2% sea (solid) and 11% sea (dashed), with $m(d')$ = 4 GeV (upper) and $m(d')$ = 5 GeV (lower). Similar results are found whether $m(u')$ = 2 or 4 GeV.

in explaining this changing value of $\langle y \rangle$, whereas model A clearly shows the general effect for $m(d')$ = 4 or 5 GeV.

In models such as A, B, D, and E this effect occurs because of the coupling $(u, d')_R$. In antineutrino scattering the ordinary $(u, d)_L$ coupling leads to a $(1-y)^2$ dependence, whereas the $(u, d')_R$ coupling leads to a 1 dependence (asymptotically). Furthermore, at present energies the production of the heavy quark d' is suppressed at small y (see Sec. III and the dimuon production described later) so that the distribution is actually increasing with y. In addition, the contribution from $(u, d')_R$ will asymptotically be three times that from $(u, d)_L$, although it is much lower at present energies. Therefore, the $(u, d')_R$ coupling leads to a significant increase in the average value of y. It should also be noted that $\langle y \rangle$ is sensitive to the amount of $\bar{d}$ in the sea since that has a constant (1) y dependence also.

By contrast, in these models the new contribution in neutrino scattering, $(u', d)_R$, only contributes $\frac{1}{3}$ asymptotically, and the new $(1-y)^2$ dependence for ν is counterbalanced by the threshold suppression of small y.

The new contributions described above must appear in the cross sections for $\nu N \to \mu +$ anything. In Figs. 4 and 5 the energy dependence of σ/E [see Eq. (2.27)] is shown. Given the error bars on the current data,[36,37] it is not possible to distinguish between the models here. However, for $\bar{\nu}$ the HPWF data appear to be rising, as does model A.
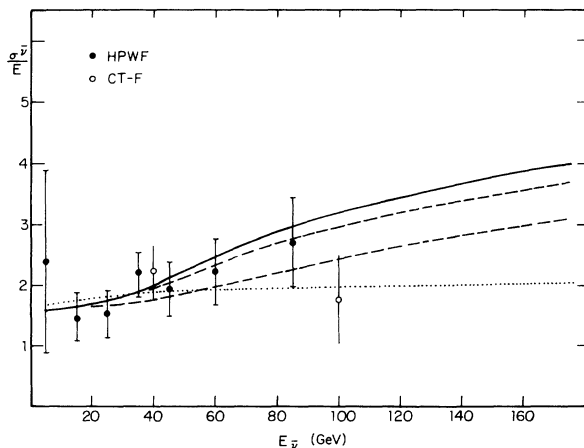
σ/E for dimuons can be obtained in Figs. 4 and 5
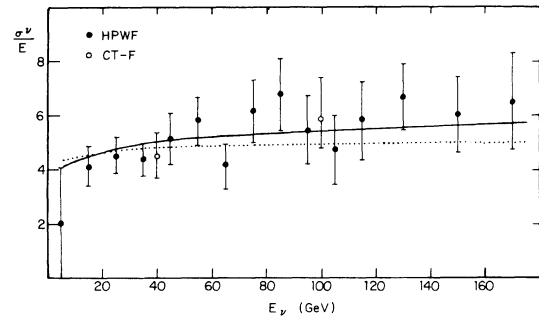

FIG. 5. The cross section for $\nu N \to \mu^- X$. Data are from Refs. 36 and 37. The curves are predictions for the standard model (dotted) and for model A (solid) where all configurations give similar results [with $m(u') = 2$ GeV somewhat higher than $m(u') = 4$ GeV]. σ/E is in arbitrary units.

by drawing a horizontal line through σ/E at $E = 5$ GeV; this line is then the zero line for dimuon cross sections.

A popular manner of displaying the cross-section data is in the ratio

$$R_c \equiv \frac{\sigma(\bar{\nu}N \to \mu^+ + X)}{\sigma(\nu N \to \mu^- + X)}. \tag{5.5}$$

Before the threshold for heavy quarks, assuming no sea, one expects $R_c = \frac{1}{3}$ [by integrating $(1-y)^2$ and 1]. With some sea contribution $R_c \gtrsim \frac{1}{3}$. This is consistent with the low-energy data. In the standard model R_c is expected to remain close to its low-energy value. Models A, B, and E have asymptotically $R_c = 1.0$ and model D, $R_c = \frac{4}{3}$. However, at the present energies these models predict R_c considerably below those values as shown in Fig. 6, which again does not distinguish the models in the energy range for which data are shown.
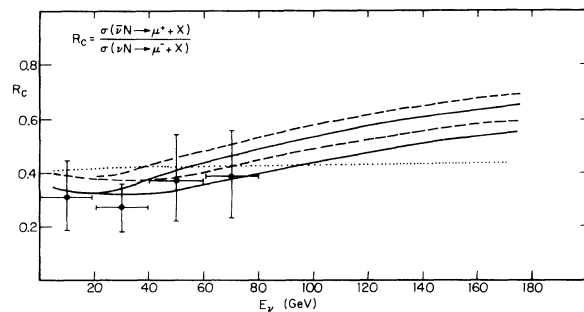
Another dramatic aspect of the HPWF data[7,36,37]

FIG. 4. The cross section for $\bar{\nu}N \to \mu^+ X$. Data are from Refs. 36 and 37. The curves are predictions for the standard model (dotted) and for model A with 2% sea, $m(d') = 4$ GeV (solid), and with 11% sea (dashed) for $m(d') = 4$ GeV (upper) and $m(d') = 5$ GeV (lower). Similar results are found whether $m(u') = 2$ or 4 GeV. σ/E is in arbitrary units.

FIG. 6. The ratio of the $\bar{\nu}$ and ν cross sections for $\nu N \to \mu X$. Data are from Ref. 36. The curves are predictions for the standard model (dotted) and for model A with 2% sea (solid) and 11% sea (dashed), and for $m(d')$ = 4 GeV (upper) and $m(d') = 5$ GeV (lower). The curves shown have $m(u') = 2$ GeV; for $m(u') = 4$ GeV all model A curves are somewhat higher.
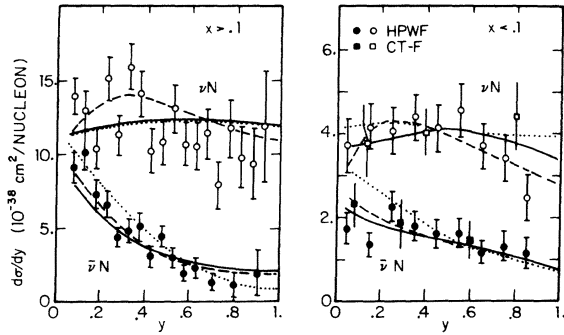
FIG. 7. The y distributions for $\nu N \to \mu X$ at small and large x. Data are from Refs. 6 and 36. The curves are predictions for the standard model (dotted) and for model A with 11% sea and with $m(u') = 4$ GeV (solid) and $m(u')$ $= 2$ GeV (dashed). Model A with 2% sea and $m(u') = 4$ GeV coincides with the solid curve for νN and with the dashed curve for $\bar{\nu}N$, $x > 0.1$, and with the dotted curve for $\bar{\nu}N$, $x < 0.1$. All the above have $m(d') = 4$ GeV. The relative normalization of ν to $\bar{\nu}$ for the data of CTF and for the theoretical curves has been adjusted within half a standard deviation of the HPWF relative normalization for better comparison of the fits.

has been the y dependence of $\bar{\nu}N \to \mu^+ + X$ at small x, shown in Fig. 7. Whereas at large x the distribution appears close to $(1 - y)^2$, for $x < 0.1$ it appears to be much flatter. There are two possible causes of this behavior (which are not exclusive): (1) the contribution of sea $\bar{d}$ quarks (which have a constant y dependence) is concentrated at small x; (2) the contribution of charmed quarks is concentrated at small x, whether they are produced off sea quarks or off valence quarks (or more likely both). As discussed in Sec. III, the kinematics restrict massive-quark production (even off valence quarks) to smaller x at present energies; and if a sharper x dependence than Eq.
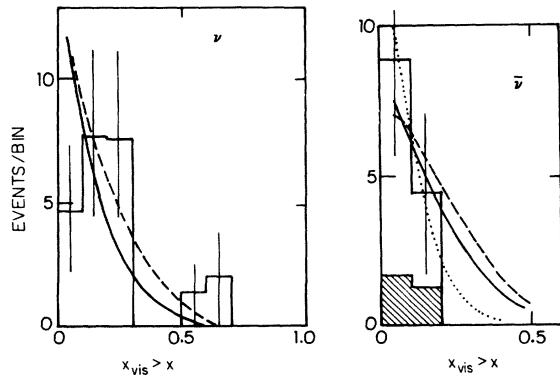

FIG. 8. The x_{vis} distributions for $\nu N \to \mu\mu X$. The data (in terms of x_{vis}) are from Refs. 11 and 12. The curves are predictions (in terms of x) for the standard model (dotted) and for model A (solid and dashed). Only the cross-hatched $\bar{\nu}$ events were obtained in a $\bar{\nu}$ run.
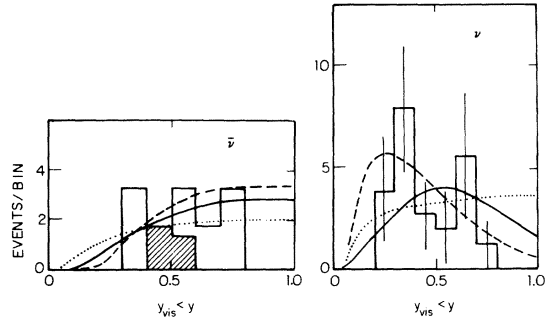

FIG. 9. The y_{vis} distributions for $\nu N \to \mu\mu X$. The data (in terms of y_{vis}) are from Refs. 11 and 12. The curves are predictions (in terms of y) for the standard model (dotted) and for model A with $m(u') = 2$ GeV (dashed) and with $m(u') = 4$ GeV (solid). Only the cross-hatched $\bar{\nu}$ events were obtained in an $\bar{\nu}$ run.

(4.3) were chosen, this effect would be even greater.

In Fig. 7, showing this y dependence for small x and large x, all models are consistent with the data. For antineutrino scattering the small x may favor model A over the standard model, but it is not decisive. For large x, perhaps the standard model does slightly better. However, it should be kept in mind that for $y \simeq 0.1$ and $x \simeq 0.1$, the x resolution in the HPWF experiment[8] is only 35%. Since small x is bounded by zero on one side but is effectively unbounded on the other side, the effect of smearing x (due to the resolution) is to shift $\langle x \rangle$ to larger values at small y where the x resolution is poor. Corrections for this effect are not easy to estimate without knowing the true x distribution at small y. The results of this effect is to make the y distribution at small x appear more flat at the same time as the y distribution at large x is made to appear sharper. It is therefore quite possible that the fits of model A are in very good agreement with the data, although one should not attempt to distinguish between models on the basis of this figure with the present data.

The currently available x, y, and $v \equiv xy$ distributions for dimuon events ($\nu N \to \mu\mu + \text{anything}$) are not very useful because of poor statistics and poor efficiency at large y. As can be seen in Figs. 8, 9, and 10, the models considered here are all easily consistent with the present data for dimuon distributions. However, with more data the neutrino y distribution and antineutrino v distribution should be quite informative.

For dimuon events (assuming they come from charmed-particle decay) it is not possible experimentally to determine x or y exactly because of the unknown energy of the outgoing neutrino, so that new quantities x_{vis} and y_{vis} are defined. If $y \equiv (E - E')/E$, where E is found by measuring the
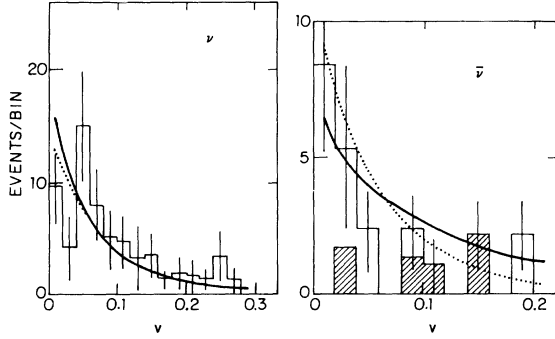
FIG. 10. The v distributions for $vN \to \mu\mu X$. The data are from Refs. 11 and 12. The curves are predictions for the standard model (dotted) and for model A (dashed and solid). Only the cross-hatched $\bar{v}$ events were obtained in an $\bar{v}$ run.

FIG. 11. The W distributions for $vN \to \mu\mu X$. The data are from Refs. 11 and 12. The curves are predictions for the standard model (dotted) and for model A with $m(u') = 4$ GeV (solid). For model A with $m(u') = 2$ GeV the v curve coincides with the standard model and the $\bar{v}$ curve with that for $m(u') = 4$ GeV. Only the cross-hatched $\bar{v}$ events obtained in an $\bar{v}$ run.

energy of all outgoing particles and $E' = E_{\mu-}$ (for neutrino scattering), then

$$y \equiv \frac{E_{had} + E_{\mu+} + E_\nu}{E_{had} + E_{\mu-} + E_{\mu+} + E_\nu}, \tag{5.6}$$

$$y_{vis} \equiv \frac{E_{had} + E_{\mu+}}{E_{had} + E_{\mu-} + E_{\mu+}}. \tag{5.7}$$

However, this error is in general quite small, in part because E_ν appears in both the numerator and the denominator. A similar result applies for x, but the variable v was chosen because the error cancels so that $v_{vis} \equiv v$.

The x distributions for dimuon events shown in Fig. 8 are all very similar for neutrinos. For antineutrinos there are some differences, but these are more pronounced in the v distributions. The antineutrino data shown should be taken with caution since most were obtained in a neutrino run by choosing those events with momenta $p(\mu^+) > p(\mu^-)$ and are therefore a biased sample. In particular since x and y dependences do not factorize [Eq. (2.27)], one finds that both the x and y distributions are affected.

The y distributions for dimuon events shown in Fig. 9 are similar for antineutrinos, but for neutrinos the distribution could be very useful in determining the mass of a u' quark [with coupling $(u', d)_R$] if there is such a quark. If one determines $m(u')$ from the best fit to these statistically poor data, one finds $m(u') \simeq 3$ GeV, but 2 or 4 GeV cannot be ruled out. For the current data, the efficiency is small at large y.

The v distributions for dimuon events are quite different for antineutrinos (Fig. 10). Again the present data should be considered with caution since only the cross-hatched data were obtained in an antineutrino run.
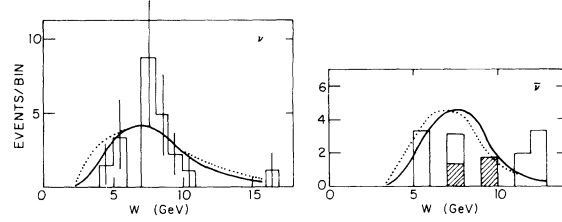
The W distributions [where W is the total invariant mass recoiling against the $\mu^-(\mu^+)$ in $v(\bar{v})$ scattering] for dimuon events are shown in Fig. 11. Since experimentally W is $W^2 = 2ME_{vis} y_{vis}(1 - x_{vis})$, there is an apparent suppression of large W because E_{vis}, y_{vis}, and $(1 - x_{vis})$ all are smaller than the true E, y, and $(1 - x)$. Furthermore, the present experiment has poor efficiency at large y. These distributions are not useful for distinguishing models, since the details of their shape are strongly dependent on the spectra of incoming neutrino energies (which are difficult to determine accurately).

In conclusion, there are significant differences in the predicted distributions for the standard four-quark model and models with right-handed currents associated with new heavy quarks. The $\langle y \rangle$ vs. E seems to favor right-handed currents. The total cross sections, single-muon y distributions, and the dimuon distributions are completely consistent with new models but do not currently rule out the four-quark model. If there are d' quarks, their mass is expected to be between 4 and 5 GeV; for u' quarks, the mass is expected to be greater than 3 GeV.

The crucial data will be the v and $\bar{v}$ dimuon rates vs. E, the $\langle y \rangle$ for $\bar{v}$ vs. E, the total cross sections at high energies, the dimuon y distribution for v, and the dimuon v distribution for $\bar{v}$. The new experiments with improved efficiency and statistics should help distinguish among these models and help estimate masses for d' and u' quarks.

ACKNOWLEDGMENTS

*Work supported in part by the National Science Foundation under Grant No. MPS75-20427.

[1]D. C. Cundy, in *Proceedings of the XVII International Conference on High Energy Physics, London, 1974,* edited by J. R. Smith (Rutherford Laboratory, Chilton, Didcot, Berkshire, England, 1974), p. IV-137; B. C. Barish, *ibid.,* p. IV-111.

[2]T. Eichten *et al.,* Phys. Lett. B46, 274 and 281 (1973).

[3]B. C. Barish *et al.,* Phys. Rev. Lett. 31, 565 (1973).

[4]A. Benvenuti *et al.,* Phys. Rev. Lett. 32, 125 (1974).

[5]A. K. Mann, in *La Physique du Neutrino à Haute Énergie,* proceedings of the Colloquium, École Polytechnique, Paris, 1975 (CNRS, Paris, 1975), p. 273.

[6]B. C. Barish, in *Proceedings of the Sixth Hawaii Topical Conference in Particle Physics, 1975,* edited by P. N. Dobson *et al.* (University of Hawaii Press, Honolulu, 1976), p. 213.

[7]B. Aubert *et al.,* Phys. Rev. Lett. 33, 984 (1974).

[8]D. Cline, talk given at the Conference on Quarks and the New Particles, 1975, University of California, Irvine (unpublished); see also A. Benvenuti *et al.,* Phys. Rev. Lett. 36, 1478 (1976).

[9]A. Benvenuti *et al.,* Phys. Rev. Lett. 34, 419 (1975).

[10]A. Benvenuti *et al.,* Phys. Rev. Lett. 35, 1199 (1975).

[11]A. Benvenuti *et al.,* Phys. Rev. Lett. 35, 1203 (1975).

[12]A. Benvenuti *et al.,* Phys. Rev. Lett. 35, 1249 (1975).

[13]B. C. Barish, in *La Physique du Neutrino à Haute Énergie,* proceedings of the Colloquium, École Polytechnique, Paris, 1975 (CNRS, Paris, 1975), p. 131.

[14]L. N. Chang, E. Derman, and J. N. Ng, Phys. Rev. Lett. 35, 6 (1975).

[15]C. H. Albright, Phys. Rev. D 12, 1319 (1975).

[16]A. Pais and S. B. Treiman, Phys. Rev. Lett. 35, 1206 (1975).

[17]S. L. Glashow, J. Iliopoulos, and L. Maiani, Phys. Rev. D 2, 1285 (1970).

[18]J. J. Aubert *et al.,* Phys. Rev. Lett. 33, 1404 (1974).

[19]J.-E. Augustin *et al.,* Phys. Rev. Lett. 33, 1406 (1974).

[20]M. Barnett, Phys. Rev. Lett. 34, 41 (1975).

[21]M. Barnett, Phys. Rev. D 11, 3246 (1975).

[22]M. Barnett, Phys. Rev. D 13, 671 (1976); this paper lists many other references also.

[23]A. De Rújula *et al.,* Phys. Rev. Lett. 35, 69 (1975).

[24]A. De Rújula *et al.,* Phys. Rev. D 12, 3589 (1975).

[25]R. L. Kingsley *et al.,* Phys. Rev. D 12, 2768 (1975).

[26]H. Fritzsch *et al.,* Phys. Lett. 59B, 256 (1975).

[27]S. Pakvasa *et al.,* Phys. Rev. Lett. 35, 703 (1975).

[28]A. De Rújula *et al.,* Rev. Mod. Phys. 46, 391 (1974).

[29]M. B. Einhorn and B. W. Lee, Phys. Rev. D 13, 43 (1976).

[30]V. Barger *et al.,* Phys. Rev. Lett. 35, 692 (1975); Nucl. Phys. B102, 439 (1976); SLAC Report No. SLAC-PUB-1688 (unpublished).

[31]Evidence that quarks in the nucleon are quasifree can be obtained by replacing m_c^2 in Eq. (2.5) with $\Delta \approx$ binding energy and seeing that scaling is found at very low energies so that Δ is quite small ($\Delta \lesssim 0.1$ GeV). It should be noted that although heavy quarks are being produced, it is still the light quark (which is struck) which must be quasifree. We thank R. Feynman for suggesting this argument.

[32]The parton model for light quarks is discussed by R. P. Feynman, in *Proceedings of the Third International Conference on High-Energy Collisions, Stony Brook, 1969,* edited by C. N. Yang *et al.* (Gordon and Breach, New York, 1969). The parton model for heavy quarks as presented here was first discussed by H. Georgi and H. D. Politzer, Harvard reports, 1975 and 1976 (unpublished).

[33]Here we follow S. Adler, in *Proceedings of the Sixth Hawaii Topical Conference in Particle Physics, 1975,* edited by P. N. Dobson *et al.* (University of Hawaii Press, Honolulu, 1976), p. 5.

[34]C. G. Callan and D. J. Gross, Phys. Rev. Lett. 22, 156 (1969).

[35]M. Gaillard, B. W. Lee, and J. Rosner, Rev. Mod. Phys. 47, 277 (1975).

[36]D. Cline, rapporteur's report given at the International Conference on High Energy Physics, Palermo, Sicily, 1975 (unpublished); see also A. Benvenuti *et al.,* Phys. Rev. Lett. (to be published) and M. Barnett, *ibid.* 36, 1163 (1976).

[37]B. C. Barish *et al.,* Phys. Rev. Lett. 35, 1316 (1975).